

# Feedback models in galaxy simulations and probing their impact by cosmological hydrodynamic simulations

Kentaro Nagamine<sup>1,2,3</sup>

<sup>1</sup>Theoretical Astrophysics Group, Department of Earth and Space Science,  
Graduate School of Science, Osaka University  
1-1 Machikaneyama-cho, Toyonaka, Osaka, 560-0043, Japan

<sup>2</sup>Department of Physics & Astronomy, University of Nevada, Las Vegas  
4505 S. Maryland Pkwy, Las Vegas, NV 89154-4002, USA

<sup>3</sup>Kavli IPMU, The University of Tokyo, 5-1-5 Kashiwanoha, Kashiwa, Chiba, 277-8583, Japan  
email: [kn@astro-osaka.jp](mailto:kn@astro-osaka.jp)

**Abstract.** Feedback effects generated by supernovae (SNe) and active galactic nuclei (AGNs) are pivotal in shaping the evolution of galaxies and their present-day structures. However, our understanding of the specific mechanisms operating at galactic scales, as well as their impact on circum-galactic medium (CGM) and intergalactic medium (IGM), remains incomplete. Galaxy formation simulations encounter challenges in resolving sub-parsec scales, necessitating the implementation of subgrid models to capture the physics occurring at smaller scales. In this article, we provide an overview of the ongoing efforts to develop more physically grounded feedback models. We discuss the pursuit of pushing simulation resolution to its limits in galaxy simulations and the rigorous testing of galaxy formation codes through participation in the AGORA code comparison project. Additionally, we delve into techniques for investigating the impact of feedback using cosmological hydrodynamic simulations, specifically through Ly $\alpha$  absorption and CGM/IGM tomography. Furthermore, we outline our future research directions within this field and highlight the progress made by comparing our simulation results with observational data.

**Keywords.** cosmology: theory, galaxies: formation, galaxies: evolution, galaxies: ISM, galaxies: high-redshift, hydrodynamics

---

## 1. Introduction

Feedback processes from supernovae (SNe) and active galactic nuclei (AGNs) have a significant impact on the regulation of galaxy formation and evolution. The prevailing consensus suggests that AGN feedback primarily acts to suppress star formation in massive galaxies at lower redshifts, whereas SN feedback predominantly affects star formation in low-mass galaxies at higher redshifts. As a result, this interplay between feedback mechanisms contributes to the observed peak in the stellar-to-halo mass relation (Behroozi et al. 2013).

High-redshift galaxies serve as excellent testbeds for examining feedback models due to the numerous intriguing physical processes taking place within them. In Figure 1, we present a schematic diagram encapsulates some of these processes. At high redshifts, low-metallicity gas streams into dark matter halos through narrow, cold flows, providing ample fuel for star formation (Kereš et al. 2005; Wright et al. 2021). However, as we transition towards lower redshifts ( $z \lesssim 2$ ), gas accretion shifts to the hot mode, and prominent cold streams diminishes in simulations (Faucher-Giguère et al. 2011; Nelson et al. 2016). The cosmic star formation rate density (SFRD) exhibits a broad peak around  $z \simeq 3 - 5$  (e.g., Nagamine et al. 2000; Nagamine et al. 2004, 2006; Kistler et al. 2009;

Madau & Dickinson 2014, and references therein), with the rising SFRD at high redshifts driven by the active formation of dark matter halos and galaxies through gravitational instability (Schaye et al. 2010). Observations employing instruments like ALMA have provided valuable insights into the emission lines expected from high-redshift galaxies, including Ly $\alpha$ , [C II], [O III] lines (e.g., Smit et al. 2018; Hashimoto et al. 2018, 2019). These observations suggest the presence of very early onset of star formation at  $z \sim 15$ .

The escape fraction ( $f_{\text{esc}}$ ) of ionizing and ultraviolet (UV) photons stands as a critical physical parameter that profoundly influences the radiative characteristics of high-redshift galaxies. However, estimating  $f_{\text{esc}}$  observationally is challenging, and only a limited number of approximate measurements have been made. Hence, it is desirable to directly predict  $f_{\text{esc}}$  for different types of galaxies using hydrodynamic simulations of galaxy formation (e.g., Cen 2003; Razoumov & Sommer-Larsen 2006; Gnedin et al. 2008; Wise & Cen 2009; Yajima et al. 2017). To make reliable predictions of  $f_{\text{esc}}$ , accurate computations of interstellar medium (ISM) structure and, thus, the attainment of high resolution are indispensable. Furthermore, understanding the intricate details of  $f_{\text{esc}}$  holds significant importance in determining whether the reionization of the universe favors the "Early" or "Late" scenarios (e.g., Finkelstein et al. 2019; Naidu et al. 2020). By conducting in-depth studies on the escape fraction, we can gain valuable insights into the processes contributing to the ionization state of the universe and the timing of reionization events. Such investigations provide crucial information for comprehending the complex interplay between galaxies, their radiation, and the overall evolution of the early universe.

## 2. Feedback models in galaxy formation simulations

In early cosmological hydrodynamic simulations, SN feedback was often simplified by injecting thermal energy on large scales ( $> \text{kpc}$ ) (Cen & Ostriker 1992; Katz 1992; Katz et al. 1996; Cen & Ostriker 1999). However, this approach faced challenges in low-resolution simulations, as the injected thermal energy would rapidly dissipate through radiation due to the inability to resolve the detailed Sedov-Taylor phase of each SN or collective superbubble. This issue, known as the overcooling problem, posed a significant hurdle. To overcome the overcooling problem, effective models of SN feedback have been developed, employing various strategies within galaxy formation simulations. These strategies include: (i) Ignoring and bypassing unresolved scales; (ii) Scaling up the energy dynamics to a resolvable scale by considering cumulative energies; or (iii) Modeling physics on unresolved scales via subgrid models.

As examples of method (i), the "delayed cooling" model temporarily ignores the cooling after a supernova event to enhance the impact of thermal feedback (Thacker & Couchman 2000; Stinson et al. 2006). The "constant velocity wind" model of Springel & Hernquist (2003) stochastically kicks gas particles and disables hydro forces until the wind particles exit the galaxies, within a smoothed particle hydrodynamics (SPH) code. In method (ii), the "stochastic thermal feedback" model increases the temperature of neighboring fluid elements by a certain value,  $\Delta T$  (Kay et al. 2003; Dalla Vecchia & Schaye 2012), so that the subsequent evolution of the hot bubble can be solved by a hydro solver with efficient thermal feedback. However, the choice of  $\Delta T$  remains somewhat arbitrary and uncertain. Method (iii) includes the "multiphase ISM model," where a single SPH particle is treated as a multiphase gas, and energy exchange between the hot and cold phases is accounted for using a subgrid equilibrium model (Yepes et al. 1997; Springel & Hernquist 2003; Keller et al. 2014). Another approach, as part of method (iii), involves injecting the terminal momentum of a single SN explosion based on the Sedov-Taylor

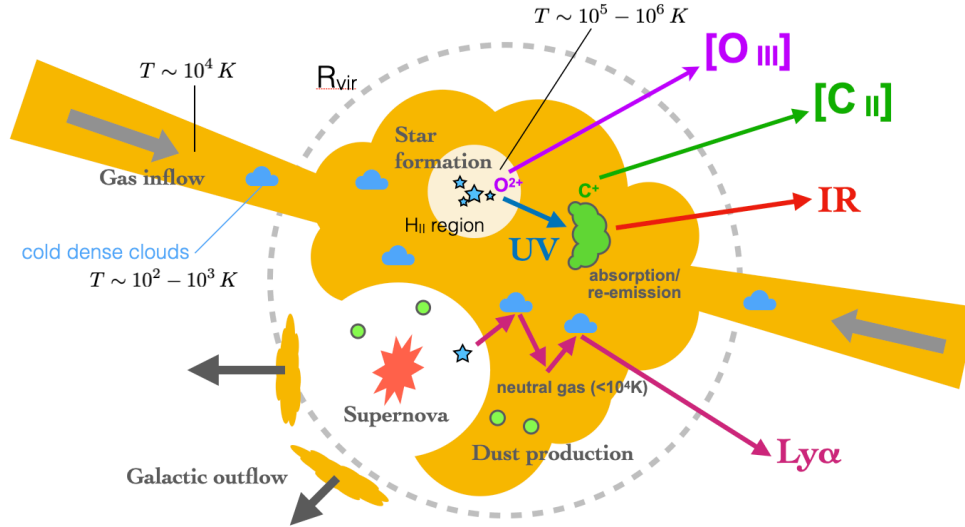


**Figure 1.** Schematic illustration of key physical processes in high-redshift galaxies. Gas inflow occurs via cold streams with  $T \sim 10^4$  K, leading to the condensation of the gas into dense clouds ( $T \sim 10^2 - 10^3$  K) through radiative cooling. Subsequent star formation gives rise to massive stars that ionize the surrounding ISM, creating H II regions. The UV radiation from massive stars impinges on the ISM surface, leading to the formation of photo-dissociation regions (PDRs), which emit infrared lines like [C II] as reprocessed radiation. These emissions from high- $z$  galaxies have been computed using cosmological zoom-in hydrodynamic simulations (e.g., Arata et al. 2019; Katz et al. 2022; Pallottini et al. 2022). In addition, prominent Ly $\alpha$  emissions are also observed from high- $z$  galaxies. After several million years, the massive stars die, resulting in the ejection of gas as galactic outflows.

solution (Kimm & Cen 2014; Hopkins et al. 2018). For further discussions on different feedback treatments, refer to Nagamine (2018) and Oku et al. (2022).

In Shimizu et al. (2019), we employed a combination of the delayed cooling model and kinetic feedback using the Sedov-Taylor self-similar solution within the GADGET3-*Osaka* code. Figure 2 presents an example of testing different SN feedback models. In the fiducial model (K30T70), we injected 30% of the SN energy as kinetic energy and 70% as thermal energy, following approaches in previous studies (e.g., Chevalier 1974; Durier & Dalla Vecchia 2012). To ensure the effectiveness of thermal feedback, cooling was temporarily disabled for the neighboring particles that received the thermal feedback energy. The gas distribution image in the face-on view of the "No-feedback" (No-FB) run exhibits a highly clumpy, cold, and dense gas distribution, with a noticeable absence of hot gas above the disk. As the fraction of thermal energy injection increases, the spiral arms become more diffuse compared to the Fiducial run. The "Stochastic thermal" (Stc-TH) and "Stochastic constant wind velocity" (Sto-CW) runs also display clumpy knots within the disk. However, the feedback effects above the disk are more pronounced in these runs, resulting in the presence of hot outflowing gas that excessively enriches the CGM. When cooling is activated in the "Cool-on" run, the gas heated by feedback rapidly

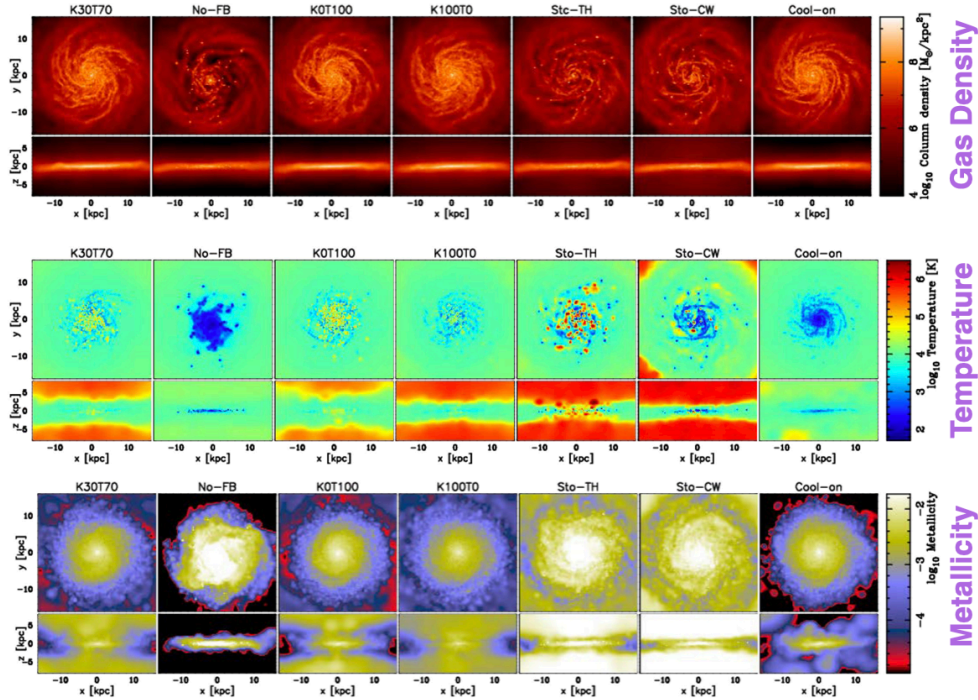


**Figure 2.** An example of testing SN feedback models in isolated galaxy simulations, showing the projected gas density, the mass-weighted temperature, and the metallicity from top to bottom rows, respectively (Shimizu et al. 2019). Within each row, the top panels show a face-on view, while the lower panel presents an edge-on view.

cools down and remains confined within the disk. Consequently, the Cool-on run exhibits similar disk features to the No-FB run. The Osaka feedback model presented in Shimizu et al. (2019) offers a valuable comparison of various SN feedback treatments. This model successfully achieves self-regulation of star formation and naturally generates galactic outflows. However, it still contained some unphysical treatments, such as the temporary disabling of cooling for effective thermal feedback.

In Oku et al. (2022), we revisited the concept of single SN remnant (SNR) and superbubble, drawing inspiration from earlier studies (Chevalier 1974; Weaver et al. 1977; Tomisaka & Ikeuchi 1986; Ostriker & McKee 1988; Martizzi et al. 2015; Kim & Ostriker 2015; Kim et al. 2017), and investigated the metallicity dependence of the terminal moment of the SN shell. Using the Eulerian hydrodynamic code ATHENA++, we extended the analytic solution for the SNR shell-formation time by (Kim & Ostriker 2015) to incorporate the effect of metallicity. Additionally, we obtained an analytic solution for the formation time of the superbubble shell. We found a universal scaling relations for the temporal evolution of momentum and radius for a superbubble when scaled by their values at the shell-formation time. Building upon these findings, we developed a SN feedback model based on the ATHENA++ simulation results. This involved employing Voronoi tessellation around each star particle and integrating it into the GADGET3-Osaka SPH code. We examined the mass/energy/metal loading factors and found that our stochastic thermal feedback model generated galactic outflows capable of transporting metals above the galactic plane while exhibiting a modest suppression of star formation. Incorporating additional mechanical feedback further suppressed star formation and improved

the agreement between simulation results and observations of the Kennicutt–Schmidt relation, considering the uncertainties in the observed data. We argued that both thermal and mechanical feedback are crucial in the SN feedback model of galaxy evolution, particularly in SPH simulations where individual SN bubbles remain unresolved.

Some simulations have made significant progress in pushing the resolution limits by focusing on low-mass galaxies. For example, Hu (2019) employed the GADGET-3 SPH simulation to study SN feedback in a dwarf galaxy residing in a dark matter halo with a virial mass of  $M_{\text{vir}} = 10^{10} M_{\odot}$ . They achieved a remarkable resolution of  $m_{\text{gas}} = 1 M_{\odot}$ , along with 0.3 pc for gravitational softening length and SPH smoothing length. Despite this high resolution, certain assumptions were still necessary, such as determining the fraction of energy given as kinetic energy and determining the number of SPH particles that receive the feedback energy. Nonetheless, they successfully simulated the formation of superbubbles with sizes of a few hundred parsecs and investigated their breakout from the galactic disk. Similarly, Ma et al. (2020) conducted simulations of dwarf galaxy formation during the reionization epoch using cosmological zoom-in simulations with the FIRE-2 GIZMO. They focused on a halo with a virial mass of  $M_{\text{vir}} = 3.7 \times 10^{10} M_{\odot}$  and achieved a mass resolution of  $m_{\text{gas}} = 100 M_{\odot}$  and a spatial resolution of approximately one parsec. They examined the location of star formation within these high-redshift dwarf galaxies in relation to the superbubbles walls and observed significant spatio-temporal variations in the escape fraction of ionizing photons. These findings are in line with previous studies by Wise & Cen (cf. 2009); Kimm & Cen (cf. 2014). As simulations continue to improve in mass resolution, approaching a "star-by-star" level, it becomes necessary to devise methods for stochastically sampling the initial mass function (IMF) for the star formation model. Several studies, including Ploeckinger et al. (2014); Hu (2019); Hirai et al. (2021), have explored this approach, but further investigation is needed to understand its impact on feedback processes as well as the overall galaxy evolution.

### 3. The AGORA code comparison project

Conducting code comparison projects is indeed an important approach to test and improve galaxy formation codes. Several notable projects have been undertaken in this regard, including the Santa Barbara cluster comparison project (Frenk et al. 1999), the Aquila project (Scannapieco et al. 2012), the nIFTy project (Knebe et al. 2015), and the AGORA project (Kim et al. 2014, 2016; Roca-Fàbrega et al. 2021). These initiatives bring together different research groups to systematically compare their simulation results, exchange ideas, identify strengths and weaknesses, and foster improvements in galaxy formation modeling.

The Santa Barbara cluster comparison project played a crucial role in highlighting the diverse results obtained from different hydrodynamic schemes and the issue of spurious entropy generation in SPH codes. This project had a profound impact on the development of new SPH schemes that could better resolve shocks, such as the density-independent scheme (Saitoh & Makino 2013) and more general formulations based on Lagrangian-based derivations (Springel & Hernquist 2002; Hopkins 2013). These improved SPH schemes offer enhanced stability and shock resolution compared to traditional versions. The incorporation of these new schemes has led to significant improvements in the fidelity of SPH simulations, addressing some of the earlier challenges and limitations associated with spurious entropy generation.

The Aquila comparison project focused on investigating code-to-code variations in galactic properties at  $z = 0$ , including stellar mass, size, morphology, and gas content.

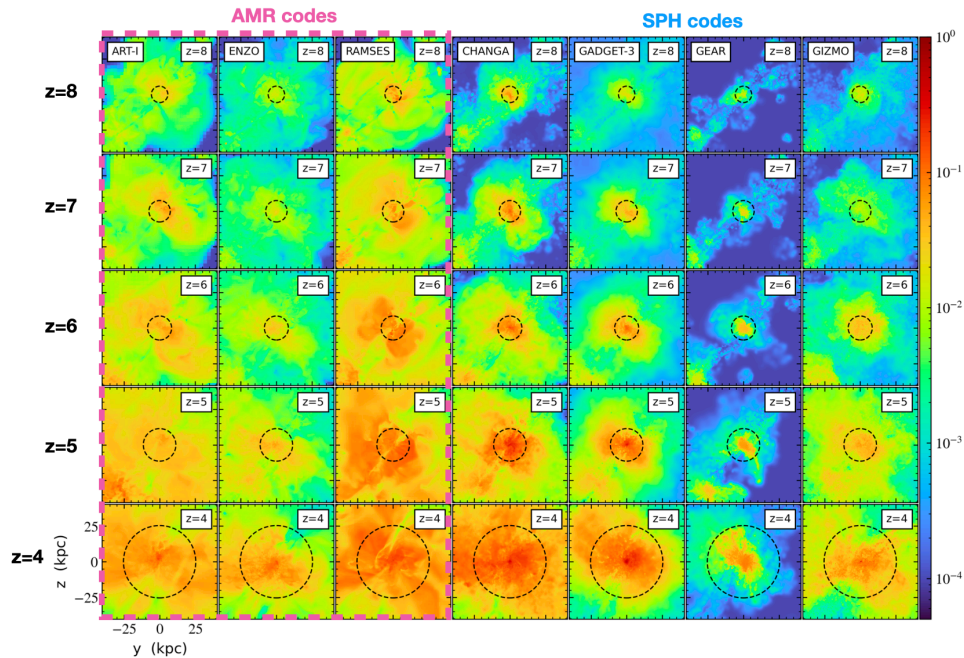


**Figure 3.** Comparison of projected (density-square-weighted) metallicity of seven different code from  $z = 8$  to  $z = 4$ . Adapted from Fig. 18 of (Roca-Fàbrega et al. 2021).

The project concluded that, due to different feedback prescriptions employed in the simulations, the models were not yet capable of uniquely predicting galactic properties, even when the assembly history of dark matter halos was the same. This highlights the importance of refining and calibrating feedback models to achieve more accurate and consistent predictions.

The AGORA project (Assembling Galaxies of Resolved Anatomy) (†) was designed to enable a more controlled environment for galaxy formation simulations. The project brought together multiple simulation codes, encompassing SPH, AMR, and moving mesh methods, and aimed to achieve consistent results by implementing common astrophysics setups. To establish a common baseline for comparison, the AGORA project initiated rigorous calibration steps that included adopting a common star formation recipe and utilizing the same Grackle cooling module (Smith et al. 2017) across all participating codes.

With these standardized astrophysics setup, the AGORA project demonstrated more consistent behaviors among the different simulation codes. Kim et al. (2016) concluded that modern high-resolution galaxy formation simulations are primarily influenced by the input physics, such as feedback prescriptions, rather than intrinsic differences in numerical schemes.

Building upon these findings, Roca-Fàbrega et al. (2021) extended the comparison to cosmological zoom-in hydro simulations, and seven contemporary astrophysical simulation codes (ART-I, ENZO, RAMSES, CHANGA, GADGET-3, GEAR, and GIZMO) were compared. The comparison process involved four systematic calibration steps, starting from a simple adiabatic run without cooling and star formation, and gradually incorpo-

† <https://sites.google.com/site/santacruzcomparisonproject/>

rating cooling, heating, and star formation in subsequent steps. In the final step, each code was tasked to reproduce a stellar mass of  $\sim 10^9 M_\odot$  at  $z = 4$  within a halo that would grow to  $10^{12} M_\odot$  by  $z = 0$ , employing code-specific SN feedback recipes.

With a physical resolution of  $\lesssim 100$  pc at  $z = 4$ , the participating codes demonstrated a general agreement on gas and stellar properties. However, interesting differences emerged in the temperature and chemical enrichment of the CGM due to variations in feedback treatments, as illustrated in Fig. 3, and Strawn et al. (2023, in preparation). These results emphasized the need for further refinement and constraint of SN and AGN feedback models through comprehensive comparisons with a wide range of observations.

Overall, the AGORA project provides a valuable framework for comparing simulation codes, promoting a deeper understanding of their similarities, differences, and areas of improvement. It highlighted the importance of standardized astrophysics setups and the ongoing development of more accurate and constrained feedback models for advancing our understanding of galaxy formation and evolution.

#### 4. Probing the impact of feedback by cosmological simulations

It is crucial to complement studies of feedback in isolated galaxies and zoom-in simulations with large-scale cosmological hydrodynamic simulations. These simulations offer the advantage of larger box sizes and a broader sample of galaxies, enabling researchers to investigate important galaxy statistics such as the galaxy stellar mass/luminosity functions and the stellar-to-halo-mass ratio (see the contribution by R. Somerville in these proceedings).

In addition to galaxies, we would also like to probe the distribution of diffuse baryons via absorption and emission lines. For example, the distribution of neutral hydrogen (HI) probed by the Ly $\alpha$  forest (e.g., Weymann et al. 1981; Cowie et al. 1995; Rauch 1998) reflects the strength of UV background radiation field and the local ionizing radiation. We anticipate that the impact of feedback is imprinted in CGM/IGM (Cen et al. 1994; Hernquist et al. 1996; Miralda-Escudé et al. 1996; Zhang et al. 1997, 1998; Theuns et al. 2002; Cen et al. 2005; Kollmeier et al. 2006). The Ly $\alpha$  forest serves as a powerful tool for cosmological studies and has been used to constrain cosmological parameters and the matter power spectrum (Weinberg et al. 1998; Croft et al. 1998; McDonald et al. 2006; Iršič et al. 2017), as well as to investigate the mass of warm dark matter particles or neutrinos (e.g. Viel et al. 2005, 2013; Palanque-Delabrouille et al. 2015). This line of research is also related to the unresolved ‘Missing baryon problem’ (Cen & Ostriker 1999; Nicastro et al. 2005; Shull et al. 2012; de Graaff et al. 2019), which refers to the challenge of observationally accounting for the entire cosmic baryon content.

IGM tomography represents an enhanced version of the Ly $\alpha$  forest technique, enabling the generation of three-dimensional contour maps of HI density in the IGM. This advanced approach utilizes a larger sample of star-forming galaxies as background sources, in addition to quasar sight-lines, to reconstruct the spatial distribution of HI gas in three dimensions. Several groups have already demonstrated the feasibility of this approach (e.g., Lee et al. 2014, 2018; Cai et al. 2016; Mukae et al. 2020), and massive protoclusters at redshifts  $z = 2 - 3$  have been identified (Lee et al. 2016; Cai et al. 2017). Moreover, this technique enables the derivation of the correlation between galaxy overdensity and HI overdensity, providing valuable insights into the relationship between galaxies/AGNs and the surrounding HI gas (Mukae et al. 2017; Liang et al. 2021; Momose et al. 2021).

The scientific objectives of IGM tomography are: (i) to characterize the cosmic web at  $z > 2$ , (ii) to study the association between galaxies/AGNs and HI gas, and (iii) to identify protoclusters and voids in an *unbiased* manner.

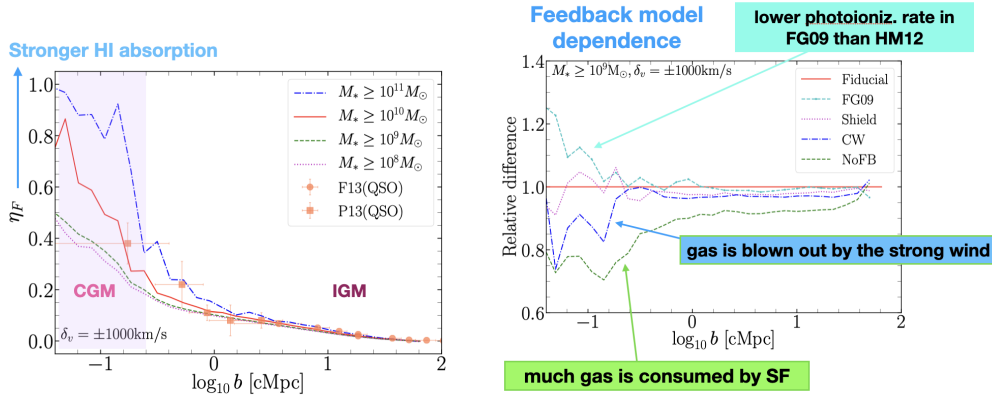


**Figure 4.** *Left:* Ly $\alpha$  flux contrast as a function of impact parameter from nearby galaxies. The data points are from Font-Ribera et al. (2013, orange filled circle; F13) and Prochaska et al. (2013, orange filled square; P13). *Right:* Relative difference in the flux contrast from the Fiducial model, showcasing runs with different feedback and UVB treatments. Both figures are adapted from Nagamine et al. (2021).

As a pathfinder to the IGM tomography studies by the Subaru PFS (Takada et al. 2014; Greene et al. 2022) and upcoming observations by the JWST/TMT/ELT, Nagamine et al. (2021) investigated the impact of feedback on basic Ly $\alpha$  forest statistics by creating a light-cone data set at  $z = 2 - 3$  and generating a mock Ly $\alpha$  forest data. They used five cosmological hydro simulations by **GADGET3-Osaka** code with different models of feedback and UVB treatment (comoving boxsize  $L_{\text{box}} = 147.6 \text{ Mpc}$ , particle number  $N = 2 \times 512^3$ ), and examined the 1D flux probability distribution function, 1D flux power spectrum, flux contrast vs. impact parameter from galaxies, and HI-galaxy cross-correlation. The flux contrast is defined as  $\eta_F \equiv -\delta_F = 1 - \frac{F}{\langle F \rangle}$ , where  $F$  is the transmitted flux ( $F = e^{-\tau}$ ), and  $\langle F \rangle$  is the average effective Ly $\alpha$  optical depth adjusted to the observed value (Becker & Bolton 2013). Higher  $\eta_F$  in the vicinity of galaxies means stronger absorption, i.e., more HI (left panel of Fig. 4). In other words, they found stronger HI absorption with decreasing impact parameter from galaxies, consistently with earlier simulation results (e.g., Bruscoli et al. 2003; Kollmeier et al. 2003, 2006; Meiksin et al. 2015; Turner et al. 2017; Meiksin et al. 2017; Sorini et al. 2018). Their simulation results demonstrated overall agreement with current observational data, but with some interesting discrepancies of about 30% on small scales that are due to different treatments of feedback and UVB, or varying observational conditions (right panel of Fig. 4). The massive galaxies with  $M_* \geq 10^{10} M_\odot$  strongly contribute to the flux contrast signal (left panel of Fig. 4), while lower-mass galaxies in the range of  $M_* \approx 10^8 - 10^{10} M_\odot$  dilute the flux contrast signal from massive galaxies when averaged over the entire galaxy sample. The variations in  $\eta_F$  on scales of  $< 1 \text{ Mpc}$  can be probed with future IGM tomography surveys with dense background source sampling by JWST/ELT/TMT. On larger scales, the average flux contrast smoothly connects to the IGM level, supporting the spherical infall model and concordance  $\Lambda$  cold dark matter model, as also found by Meiksin et al. (2017); Sorini et al. (2018). Interestingly, Sorini et al. (2020) reported negligible impact of AGN feedback on the flux contrast, suggesting that stellar feedback primarily determines the average physical properties of CGM at  $z = 2 - 3$ . However, further investigation in simulations incorporating AGN feedback is warranted to confirm this finding (cf. Tillman et al. 2022).

In addition to HI distribution, metal distribution can also be probed by emission and



absorption lines. For example, the MEGAFLOW project has observed Mg II lines in both absorption and emission in the galactic wind region of  $z \sim 0.7$  galaxy (Zabl et al. 2020, 2021). In a different study, Nelson et al. (2021) computed the resonantly scattered Mg II emission from the TNG50 simulation. Their analysis indicates that the simulated galaxies exhibit somewhat steeper profiles (i.e., a faster decline with increasing radii) compared to the observed data points (see their Fig. 3). However, the currently observed sources are especially bright ones that are easily detectable, therefore, further comparisons with lower mass systems are necessary in the future.

Interestingly, similar trends are observed in other emission lines, such as [C II] (Arata et al. 2020; Fujimoto et al. 2019), and Ly $\alpha$  (Zhang et al. 2020), where the simulated galaxies fail to reproduce the observed extended emission profiles. These discrepancies have interesting implications for the feedback efficiencies, such as the mass-loading factor of metals in galactic outflows (Pizzati et al. 2020), and therefore warrant further studies to constrain the efficiencies of chemical enrichment in CGM and IGM.

## 5. Summary

In this article, we reviewed various feedback treatments in galaxy simulations, and discussed our development of physically-based SN feedback models and the tests within the AGORA project using isolated galaxies and zoom-in cosmological hydrodynamic simulations. We argued that considering both thermal and kinetic modes of SN feedback is important at the current resolution level ( $\gtrsim 10$  pc). In our recent work, Oku et al. (2022) showed that the kinetic feedback suppresses star formation while stochastic thermal feedback drives strong metal outflows. Further studies on both small and large scales are crucial to fully understand the role of feedback in galaxy evolution and the chemical enrichment of CGM/IGM.

Notably there are indications that very high-resolution simulations ( $\lesssim$  pc scale) exhibit weaker winds compared to larger-scale simulations that capture the physics of galactic winds on supergalactic scales (see contributions by E. Ostriker and C.-G. Kim in this proceedings, as well as Hu 2019). Additionally, the inclusion of additional physics, such as cosmic rays and magnetic fields, will be essential for constructing more physically plausible models of star formation and feedback (e.g., Hopkins et al. 2022).

It might also be possible to constrain the physics of feedback at larger scales of circumgalactic and intergalactic scales utilizing the Ly $\alpha$  absorption by neutral hydrogen (commonly referred to as IGM tomography) and distribution of metals and dust. For example, Nagamine et al. (2021) have shown that SN feedback influences the radial distribution of H I gas and the Ly $\alpha$  flux contrast signal at  $\sim 30\%$  level. Future comparisons between simulations and the CGM/IGM tomography surveys by WEAVE, MOONS, Subaru PFS, JWST, ELT, and TMT will provide valuable insights and further constrain the physics of feedback.

I am grateful to all of my recent collaborators on the research results discussed in this article, including S. Arata, R. Cen, K. G. Lee, R. Momose, Y. Oku, L. Romano, I. Shimizu, K. Tomida, H. Yajima, and everyone in the AGORA project.

## References

- Arata, S., Yajima, H., Nagamine, K., Abe, M., & Khochfar, S. 2020, *MNRAS*, 498, 5541  
 Arata, S., Yajima, H., Nagamine, K., Li, Y., & Khochfar, S. 2019, *MNRAS*, 488, 2629  
 Becker, G. D., & Bolton, J. S. 2013, *MNRAS*, 436, 1023

- Behroozi, P. S., Wechsler, R. H., & Conroy, C. 2013, *ApJ*, 770, 57
- Bruscoli, M., Ferrara, A., Marri, S., et al. 2003, *MNRAS*, 343, L41
- Cai, Z., Fan, X., Peirani, S., et al. 2016, *ApJ*, 833, 135
- Cai, Z., Fan, X., Bian, F., et al. 2017, *ApJ*, 839, 131
- Cen, R. 2003, *ApJ*, 591, 12
- Cen, R., Miralda-Escudé, J., Ostriker, J. P., & Rauch, M. 1994, *ApJL*, 437, L9
- Cen, R., Nagamine, K., & Ostriker, J. P. 2005, *ApJ*, 635, 86
- Cen, R., & Ostriker, J. P. 1992, *ApJL*, 399, L113
- . 1999, *ApJ*, 514, 1
- Chevalier, R. A. 1974, *ApJ*, 188, 501
- Cowie, L. L., Songaila, A., Kim, T.-S., & Hu, E. M. 1995, *AJ*, 109, 1522
- Croft, R. A. C., Weinberg, D. H., Katz, N., & Hernquist, L. 1998, *ApJ*, 495, 44
- Dalla Vecchia, C., & Schaye, J. 2012, *MNRAS*, 426, 140
- de Graaff, A., Cai, Y.-C., Heymans, C., & Peacock, J. A. 2019, *A&A*, 624, A48
- Durier, F., & Dalla Vecchia, C. 2012, *MNRAS*, 419, 465
- Faucher-Giguère, C.-A., Kereš, D., & Ma, C.-P. 2011, *MNRAS*, 417, 2982
- Finkelstein, S. L., D’Aloisio, A., Paardekooper, J.-P., et al. 2019, *ApJ*, 879, 36
- Font-Ribera, A., Arnau, E., Miralda-Escudé, J., et al. 2013, *JCAP*, 5, 018
- Frenk, C. S., White, S. D. M., Bode, P., et al. 1999, *ApJ*, 525, 554
- Fujimoto, S., Ouchi, M., Ferrara, A., et al. 2019, *ApJ*, 887, 107
- Gnedin, N. Y., Kravtsov, A. V., & Chen, H. 2008, *ApJ*, 672, 765
- Greene, J., Bezanson, R., Ouchi, M., Silverman, J., & the PFS Galaxy Evolution Working Group. 2022, arXiv e-prints, arXiv:2206.14908
- Hashimoto, T., Laporte, N., Mawatari, K., et al. 2018, *Nature*, 557, 392
- Hashimoto, T., Inoue, A. K., Mawatari, K., et al. 2019, *PASJ*, 71, 71
- Hernquist, L., Katz, N., Weinberg, D. H., & Miralda-Escudé, J. 1996, *ApJL*, 457, L51
- Hirai, Y., Fujii, M. S., & Saitoh, T. R. 2021, *PASJ*, 73, 1036
- Hopkins, P. F. 2013, *MNRAS*, 428, 2840
- Hopkins, P. F., Butsky, I. S., Panopoulou, G. V., et al. 2022, *MNRAS*, 516, 3470
- Hopkins, P. F., Wetzel, A., Kereš, D., et al. 2018, *MNRAS*, 477, 1578
- Hu, C.-Y. 2019, *MNRAS*, 483, 3363
- Iršič, V., Viel, M., Berg, T. A. M., et al. 2017, *MNRAS*, 466, 4332
- Katz, H., Rosdahl, J., Kimm, T., et al. 2022, *MNRAS*, 510, 5603
- Katz, N. 1992, *ApJ*, 391, 502
- Katz, N., Weinberg, D. H., & Hernquist, L. 1996, *ApJS*, 105, 19
- Kay, S. T., Thomas, P. A., & Theuns, T. 2003, *MNRAS*, 343, 608
- Keller, B. W., Wadsley, J., Benincasa, S. M., & Couchman, H. M. P. 2014, *MNRAS*, 442, 3013
- Kereš, D., Katz, N., Weinberg, D. H., & Davé, R. 2005, *MNRAS*, 363, 2
- Kim, C.-G., & Ostriker, E. C. 2015, *ApJ*, 802, 99
- Kim, C.-G., Ostriker, E. C., & Raileanu, R. 2017, *ApJ*, 834, 25
- Kim, J.-H., Abel, T., Agertz, O., et al. 2014, *ApJS*, 210, 14
- Kim, J.-h., Agertz, O., Teyssier, R., et al. 2016, *ApJ*, 833, 202
- Kimm, T., & Cen, R. 2014, *ApJ*, 788, 121
- Kistler, M. D., Yüksel, H., Beacom, J. F., Hopkins, A. M., & Wyithe, J. S. B. 2009, *ApJL*, 705, L104
- Knebe, A., Pearce, F. R., Thomas, P. A., et al. 2015, *MNRAS*, 451, 4029
- Kollmeier, J. A., Miralda-Escudé, J., Cen, R., & Ostriker, J. P. 2006, *ApJ*, 638, 52
- Kollmeier, J. A., Weinberg, D. H., Davé, R., & Katz, N. 2003, *ApJ*, 594, 75
- Lee, K.-G., Hennawi, J. F., Stark, C., et al. 2014, *ApJL*, 795, L12
- Lee, K.-G., Hennawi, J. F., White, M., et al. 2016, *ApJ*, 817, 160
- Lee, K.-G., Krolewski, A., White, M., et al. 2018, *ApJS*, 237, 31
- Liang, Y., Kashikawa, N., Cai, Z., et al. 2021, *ApJ*, 907, 3
- Ma, X., Quataert, E., Wetzel, A., et al. 2020, arXiv e-prints, arXiv:2003.05945
- Madau, P., & Dickinson, M. 2014, *ARA&A*, 52, 415

- Martizzi, D., Faucher-Giguère, C.-A., & Quataert, E. 2015, *MNRAS*, 450, 504
- McDonald, P., Seljak, U., Burles, S., et al. 2006, *ApJS*, 163, 80
- Meiksin, A., Bolton, J. S., & Puchwein, E. 2017, *MNRAS*, 468, 1893
- Meiksin, A., Bolton, J. S., & Tittley, E. R. 2015, *MNRAS*, 453, 899
- Miralda-Escudé, J., Cen, R., Ostriker, J. P., & Rauch, M. 1996, *ApJ*, 471, 582
- Momose, R., Shimizu, I., Nagamine, K., et al. 2021, *ApJ*, 911, 98
- Mukae, S., Ouchi, M., Kakiichi, K., et al. 2017, *ApJ*, 835, 281
- Mukae, S., Ouchi, M., Cai, Z., et al. 2020, *ApJ*, 896, 45
- Nagamine, K. 2018, *The Encyclopedia of Cosmology. Volume 2: Numerical Simulations in Cosmology, Vol. 2 (World Scientific Publishing)*, doi:10.1142/9496-vol2
- Nagamine, K., Cen, R., Hernquist, L., Ostriker, J. P., & Springel, V. 2004, *ApJ*, 610, 45
- Nagamine, K., Cen, R., & Ostriker, J. P. 2000, *ApJ*, 541, 25
- Nagamine, K., Ostriker, J. P., Fukugita, M., & Cen, R. 2006, *ApJ*, 653, 881
- Nagamine, K., Shimizu, I., Fujita, K., et al. 2021, *ApJ*, 914, 66
- Naidu, R. P., Tacchella, S., Mason, C. A., et al. 2020, *ApJ*, 892, 109
- Nelson, D., Byrohl, C., Peroux, C., Rubin, K. H. R., & Burchett, J. N. 2021, *MNRAS*, 507, 4445
- Nelson, D., Genel, S., Pillepich, A., et al. 2016, *MNRAS*, 460, 2881
- Nicastro, F., Mathur, S., Elvis, M., et al. 2005, *Nature*, 433, 495
- Oku, Y., Tomida, K., Nagamine, K., Shimizu, I., & Cen, R. 2022, *ApJS*, 262, 9
- Ostriker, J. P., & McKee, C. F. 1988, *Reviews of Modern Physics*, 60, 1
- Palanque-Delabrouille, N., Yèche, C., Lesgourgues, J., et al. 2015, *JCAP*, 2015, 045
- Pallottini, A., Ferrara, A., Gallerani, S., et al. 2022, *MNRAS*, 513, 5621
- Pizzati, E., Ferrara, A., Pallottini, A., et al. 2020, *MNRAS*, 495, 160
- Ploeckinger, S., Hensler, G., Recchi, S., Mitchell, N., & Kroupa, P. 2014, *MNRAS*, 437, 3980
- Prochaska, J. X., Hennawi, J. F., Lee, K.-G., et al. 2013, *ApJ*, 776, 136
- Rauch, M. 1998, *ARA&A*, 36, 267
- Razoumov, A. O., & Sommer-Larsen, J. 2006, *ApJL*, 651, L89
- Roca-Fàbrega, S., Kim, J.-H., Hausammann, L., et al. 2021, *ApJ*, 917, 64
- Saitoh, T. R., & Makino, J. 2013, *ApJ*, 768, 44
- Scannapieco, C., Wadepuhl, M., Parry, O. H., et al. 2012, *MNRAS*, 423, 1726
- Schaye, J., Dalla Vecchia, C., Booth, C. M., et al. 2010, *MNRAS*, 402, 1536
- Shimizu, I., Todoroki, K., Yajima, H., & Nagamine, K. 2019, *MNRAS*, 484, 2632
- Shull, J. M., Smith, B. D., & Danforth, C. W. 2012, *ApJ*, 759, 23
- Smit, R., Bouwens, R. J., Carniani, S., et al. 2018, *Nature*, 553, 178
- Smith, B. D., Bryan, G. L., Glover, S. C. O., et al. 2017, *MNRAS*, 466, 2217
- Sorini, D., Davé, R., & Anglés-Alcázar, D. 2020, *MNRAS*, 499, 2760
- Sorini, D., Oñorbe, J., Hennawi, J. F., & Lukić, Z. 2018, *ApJ*, 859, 125
- Springel, V., & Hernquist, L. 2002, *MNRAS*, 333, 649
- . 2003, *MNRAS*, 339, 289
- Stinson, G., Seth, A., Katz, N., et al. 2006, *MNRAS*, 373, 1074
- Takada, M., Ellis, R. S., Chiba, M., et al. 2014, *PASJ*, 66, R1
- Thacker, R. J., & Couchman, H. M. P. 2000, *ApJ*, 545, 728
- Theuns, T., Viel, M., Kay, S., et al. 2002, *ApJL*, 578, L5
- Tillman, M. T., Burkhardt, B., Tonnesen, S., et al. 2022, arXiv e-prints, arXiv:2210.02467
- Tomisaka, K., & Ikeuchi, S. 1986, *PASJ*, 38, 697
- Turner, M. L., Schaye, J., Crain, R. A., et al. 2017, *MNRAS*, 471, 690
- Viel, M., Becker, G. D., Bolton, J. S., & Haehnelt, M. G. 2013, *Phys. Rev. D*, 88, 043502
- Viel, M., Lesgourgues, J., Haehnelt, M. G., Matarrese, S., & Riotto, A. 2005, *Phys. Rev. D*, 71, 063534
- Weaver, R., McCray, R., Castor, J., Shapiro, P., & Moore, R. 1977, *ApJ*, 218, 377
- Weinberg, D. H., Burles, S., Croft, R. A. C., et al. 1998, ArXiv Astrophysics e-prints, astro-ph/9810142
- Weymann, R. J., Carswell, R. F., & Smith, M. G. 1981, *ARA&A*, 19, 41
- Wise, J. H., & Cen, R. 2009, *ApJ*, 693, 984

- Wright, R. J., Lagos, C. d. P., Power, C., & Correa, C. A. 2021, *MNRAS*, 504, 5702
- Yajima, H., Nagamine, K., Zhu, Q., Khochfar, S., & Dalla Vecchia, C. 2017, *ApJ*, 846, 30
- Yepes, G., Kates, R., Khokhlov, A., & Klypin, A. 1997, *MNRAS*, 284, 235
- Zabl, J., Bouché, N. F., Schroetter, I., et al. 2020, *MNRAS*, 492, 4576
- Zabl, J., Bouché, N. F., Wisotzki, L., et al. 2021, *MNRAS*, 507, 4294
- Zhang, H., Ouchi, M., Itoh, R., et al. 2020, *ApJ*, 891, 177
- Zhang, Y., Anninos, P., Norman, M. L., & Meiksin, A. 1997, *ApJ*, 485, 496
- Zhang, Y., Meiksin, A., Anninos, P., & Norman, M. L. 1998, *ApJ*, 495, 63